JOINT EUROPEAN TORUS

JET–P(92)85

F. Porcelli
and JET Team

Collisionless Magnetic Reconnection in Laboratory Plasmas

Collisionless Magnetic Reconnection in Laboratory Plasmas

F. Porcelli and JET Team*

JET-Joint Undertaking, Culham Science Centre, OX14 3DB, Abingdon, UK

** See Annex*

Preprint of a paper to be submitted for publication in the proceedings of the
Varenna Theory Workshop, 1992

Collisionless Magnetic Reconnection in Laboratory Plasmas

F. Porcelli

JET Joint Undertaking, Abingdon, Oxon, OX14 3EA, UK.

ABSTRACT

Collisionless reconnection - considered to be a fundamental process in Astrophysics - can now be observed in laboratory plasmas close to thermonuclear breakeven conditions. In particular, because of the high temperatures which have been attained in recent experiments, this process is now thought to occur during the so-called "sawtooth" relaxation oscillations which affect the interior of a magnetically confined, current-carrying plasma. We review novel linear and nonlinear theoretical efforts applied to the understanding of sawtooth oscillations in regimes where the relaxation rate is determined by the plasma skin depth and by the ion Larmor radius, rather than by Coulomb collisions.

I. INTRODUCTION

The occurrence of magnetic field line reconnection in collisionless regimes, where electron inertia is responsible for the decoupling of the plasma motion from that of the magnetic field, has been considered for a long time to be a fundamental process in many astrophysical objects, such as for instance the low plasma density environment of the Earth's magnetotail. A discussion of the subject can be found, e.g., in a review article by Vasyliunas (1975). Now, the detailed experimental observation of collisionless reconnection in space plasmas is, of course, rather difficult. Therefore, it is quite exciting that laboratory plasmas produced by the Joint European Torus (JET) and by the Tokamak Fusion Test Reactor (TFTR) have recently entered a high electron temperature regime where collisionless reconnection can be observed. In fact, in these plasma discharges, the electron-ion collision time, τ_{ei}, is found to be comparable to, or even longer than, the relaxation time of internal plasma ("sawtooth") oscillations. Also, the ion Larmor radius is larger than the plasma skin depth (examples are discussed in Section IV below). Under these

conditions, the rate (normalized to the characteristic Alfvén time) at which magnetic reconnection can occur is determined, at least during the early stage of sawtooth relaxations, by an appropriate combination of the skin depth and of the ion Larmor radius, normalized to the macroscopic size of the reconnecting region, rather than by collisional effects.

Sawtooth oscillations in collisionless regimes will be the focus of this paper. These relaxation oscillations, first reported by von Goeler et al in 1974, are a well-known instability of magnetically confined toroidal plasmas where the poloidal magnetic field, B_ϑ, is produced by a toroidal current carried by the plasma itself. The relaxation is initiated by a helical mode with toroidal n = 1 and dominant poloidal m = 1 wave numbers (in short, an "m = 1 mode"). This mode, which breaks the toroidal symmetry of the initial equilibrium, displaces the equilibrium magnetic axis, where $q(0) < 1$, and causes magnetic surfaces to reconnect around the region where $q(r_s) = 1$. Here, $q(r) \approx rB_\varphi/RB_\vartheta$ is the magnetic helical parameter, with B_φ the toroidal field, R the torus major radius, and r the mean distance of a magnetic surface from the magnetic axis. We refer to Edwards et al (1986) and to McGuire et al (1990) for recent experimental accounts of sawteeth in JET and TFTR, respectively.

From a theoretical point of view, Wesson (1990) was the first to point out that plasmas produced by JET and by TFTR have entered a low collisionality regime for the m = 1 instability where the electron inertial term in the generalized Ohm law should start to be felt. Following an argument proposed earlier by Kadomtsev (1975), Wesson obtained a modification of Kadomtsev's scaling for the sawtooth reconnection in the collisionless regime where electron inertia dominates over resistivity in Ohm's law. Wesson's analysis was followed by a linear stability analysis of m = 1 modes including full ion Larmor radius effects (Porcelli, 1991). Both Wesson's and Porcelli's analyses indicated that magnetic reconnection in low collisionality regimes can occur on a fast time scale which compares favourably with the experimental relaxation times. However, a numerical simulation by Drake and Kleva (1991) revealed that, under the assumption of negligible ion Larmor radius (and

electron pressure gradient in Ohm's law), the nonlinear collisionless current layer collapses to a thickness which is much smaller than the plasma skin depth, bringing reconnection almost to a halt. As a consequence, Drake and Kleva concluded that electron inertia cannot, by itself, cause the fast sawtooth crash.

In Drake and Kleva's simulations, the width of the plasma flow as well as that of the current layer become extremely narrow. Now, when finite temperature effects are properly accounted for, the width of the ion flow is limited by the ion (sound) Larmor radius. In this case, the structure of the current density channel may also be affected. Then, contrary to Drake and Kleva's conclusions, it may be possible that reconnection can remain a fast process nonlinearly, as preliminary investigations by Kleva et al (1992), by Zakharov and Rogers (1992a) and by Aydemir (1992) appear to hint to.

Before concluding this section, it is worth pointing out that magnetic reconnection can occur even in the absence of a dissipative process. Indeed, the electron inertial term in the generalized Ohm law allows the transfer of magnetic energy into electron kinetic energy, while the total entropy of the system remains constant. To account for the irreversibility of the reconnection process, one should note that electrons are accelerated in a narrow layer to very large speeds along the magnetic field lines. Thus, the electron distribution function tends to become highly distorted and one can think of velocity space instabilities which would limit this tendency, introducing an effective ("anomalous") current diffusion. For instance, Drake and Kleva (1991) proposed that the extremely narrow current layer observed in their zero Larmor radius simulation is limited by a current convective instability (Mikhailovskii, 1974) which allows reconnection to proceed. Another interesting possibility is the onset of a two stream instability which would limit the parallel drift velocity of the electrons to their thermal velocity level. However, we remark that, as a matter of principle, knowledge of the eventual fate of the electron distribution may not be required in order to evaluate the reconnection rate in collisionless regimes. A relevant analogy is that of a wave

resonating with charged particles, where the Landau damping rate can be calculated without having to know where the wave energy eventually goes.

This paper is organized as follows: In Section II we discuss the linear stability theory. Nonlinear considerations are presented in Section III. In Section IV we present a comparison between theory and experiments, followed by concluding remarks.

II LINEAR THEORY

In addition to the plasmas skin depth, $d_e = c/\omega_{pe}$, with $\omega_{pe} = (4\pi ne^2/m_e)^{1/2}$, and to the "true" ion Larmor radius, $\rho_i = v_{thi}/\Omega_{ci}$, with $v_{thi} = (T_i/m_i)^{1/2}$ and $\Omega_{ci} = ZeB/m_ic$, another relevant scale length introduced by the the perturbed electron pressure gradient along the field lines is $\rho_s = c_s/\Omega_{ci}$, with $c_s = (T_e/m_i)^{1/2}$. The distance ρ_s is often referred to as the "ion sound Larmor radius". It represents the characteristic distance from a given field line over which the kinetic energy of transverse ion density oscillations is balanced by the restoring parallel force associated with the pressure perturbation of electrons moving rapidly along the field line in order to preserve quasi neutrality. Note that $\rho_s/\rho_i = \tau^{1/2}$, where $\tau = T_e/T_i$. Early investigations of linear m = 1 modes in collisionless regimes (Hazeltine and Strauss, 1978; Drake, 1978; Basu and Coppi, 1981) considered the cold ion limit, $\rho_i \rightarrow 0$, while retaining effects associated with finite ρ_s. The cold ion approximation implies that a fluid model for the ions can be assumed, while a full kinetic treatment for the electrons was employed in the mentioned early investigations. In this case the linear width of the collisionless current channel is determined by the skin depth (although the flow width extends to distances ~ ρ_s), so that the fluid ion approximation remains valid so long as $\rho_i < d_e$. Now,

$$(\rho_i/d_e) = (m_i\beta_i/2m_e)^{1/2} \qquad (1)$$

tends to be larger than unity for realistic values of the ion $\beta_i = 8\pi p_i/B^2$ parameter. Therefore, the analysis of Porcelli (1991), which is reviewed in this Section, was aimed at extending the early analyses to the regime where $\rho_i > d_e$. This extension requires a full kinetic (Vlasov) treatment of the ion dynamics,

leading to a rather involved integro-differential dispersion equation in coordinate space (see, e.g., Antonsen and Coppi, 1981). The analysis simplifies greatly in Fourier space, where an ordinary differential dispersion equation can be obtained (Pegoraro and Schep, 1986; Pegoraro et al, 1988). This simplification arises provided ion Landau damping is neglected. This, however, is a safe approximation, in so far as modes are found whose complex frequency satisfies $\omega >> k_{\|} v_{thi}$, where $k_{\|} \sim \delta/L_s$ is the parallel wavelength, with δ the layer width (normalized to the q = 1 radius), $L_s = R/s$ and $s = r_s q'(r_s)$. As for the electrons, a fluid approximation can be assumed, with the generalised Ohm law

$$\vec{E} + \frac{1}{c}\vec{V}_e \times \vec{B} = \eta \vec{J} + \frac{m_e}{n_e e^2}\left(\frac{\partial}{\partial t} + \vec{V}_e \cdot \nabla\right)\vec{J} - \frac{1}{n_e e}\nabla \cdot \vec{\vec{P}}_e \qquad (2)$$

where n_e is the electron density, $\vec{\vec{P}}_e$ is the electron stress tensor and the other terms have their usual meaning. The fluid electron model requires a closure. In the large ρ_s or ρ_i limits, it can be shown a posteriori that this closure is accomplished by the choice of an isothermal equation of state. We point out that the fluid electron approximation excludes the treatment of modes whose growth or damping may depend on Landau resonant processes. We believe, however, that only a macroscopic instability involving the bulk of the electron population should be capable of explaining such a dramatic rearrangement of the plasma configuration observed during sawtooth relaxations.

We sketch the mathematical derivation of the linear dispersion equation within the reconnection layer. For reasons of mathematical clarity, diamagnetic effects are discussed later although they are not retained explicitly in the following derivation (but can be found in Porcelli, 1991). We consider a toroidal equilibrium with negligible radial electric field and equilibrium flows. The presence of an equilibrium radial electric field, provided its gradient is not too large, will simply have the effect of introducing a Doppler shift in the m = 1 mode frequency, without affecting the growth rate (see, e.g. Ara et al, 1978). Assuming a q profile such that $1\text{-}q \geq r/R$ in the central region of the plasma column and finite magnetic shear at the q = 1 surface, we can use the ideal MHD analysis of Bussac et al (1975) to describe the plasma motion everywhere

except in the layer around the q = 1 surface where non-ideal effects become important. Perturbed quantities are assumed to vary as $\tilde{\varphi}(\vec{r},t) \approx \hat{\varphi}(x)\exp[\gamma t + i(\vartheta - \varphi)]$, with $m \neq 1$ satellite poloidal components retained in the MHD region but neglected in the layer. Here, $x = (r - r_s)/r_s$ is the distance from the q = 1 surface. The perturbed electron continuity equation gives

$$\tilde{n}_e / n_e = (en\gamma)^{-1}\nabla_{\|}\tilde{J}_{\|e}, \tag{3}$$

where $\nabla_{\|} \approx ik_{\|} = -ix/L_s$. The perturbed ion density is obtained from Vlasov's equation. In the relevant limit $\omega >> k_{\|}v_{thi}$, one finds

$$\tilde{n}_i / n_i = -L e\tilde{\phi} / T_i, \tag{4}$$

where L is a differential operator defined by $L = 1 - I_o(b)e^{-b}$, with I_o a modified Bessel function of the first kind and $b = -\rho_i^2\nabla_{\perp}^2$. Such a definition of L makes sense if $I_o(b)\,e^{-b}$ is represented by its power series. In the small ion Larmor radius limit, $b << 1$, $L \approx -\rho_i^2\nabla_{\perp}^2$ reduces to a second-order differential operator. In the opposite limit, $b >> 1$, $L \to 1$ and the perturbed ion density follows the Boltzmann response. The quasineutrality condition gives

$$L e\tilde{\phi} / T_i = (en\gamma)^{-1}\nabla_{\|}\tilde{J}_{\|e}. \tag{5}$$

The parallel component of the linearized Ohm law (2) gives

$$\tilde{E}_{\|} = \left(m_e / n_e e^2\right)(\gamma + \nu_{ei}/2)\,\tilde{J}_{\|e} - (n_e e)^{-1}\nabla_{\|}\tilde{p}_e, \tag{6}$$

where we have used $\eta_{\|} = m_e\nu_{ei}/2n_e e^2$. We set $\tilde{p}_e/p_e \approx \Gamma\tilde{n}_e/n_e$, with $\Gamma = 5/3$ for an adiabatic equation of state and $\Gamma = 1$ for an isothermal equation of state. If we now apply the operator $\nabla_{\perp}^2$ to Eq. (6), use $\tilde{E}_{\|} = -\nabla_{\|}\tilde{\phi} - (\gamma/c)\tilde{A}_{\|}$, Ampere's law $(4\pi/c)\tilde{J}_{\|} = -\nabla_{\perp}^2\tilde{A}_{\|}$ and Eq. (3) to eliminate $\tilde{n}_e/n_e$, we obtain

$$-\nabla_{\perp}^2\nabla_{\|}\tilde{\phi} + \frac{4\pi\gamma}{c^2}\tilde{J}_{\|e} = \frac{m_e}{n_e e^2}\left(\gamma + \frac{1}{2}\nu_{ei}\right)\nabla_{\perp}^2\tilde{J}_{\|e} - \frac{\Gamma T_e}{n_e e^2\gamma}\nabla_{\perp}^2\nabla_{\|}^2\tilde{J}_{\|e} \tag{7}$$

Equations (5) and (7) form a closed set for the unknowns $\tilde{\phi}$ and $\tilde{J}_{\|e}$.

Now we switch to Fourier space. Introduce $J(k) = \int_{-\infty}^{\infty}\hat{J}_{\|}(x)\exp(ikx)dx$. The differential operators transform into $\nabla_{\perp}^2 \to -r_s^2k^2$ and $\nabla_{\|} \to -L_s^{-1}(d/dk)$. L becomes an algebraic quantity: $L = 1 - I_o(\rho^2k^2)\exp(-\rho^2k^2)$, with $\rho \equiv \rho_i/r_s$. Eliminating $\phi(k)$ in Eqs. (5) and (7), we obtain the dispersion equation

$$\frac{d}{dk}\left(\Gamma\tau+\frac{1}{L}\right)\frac{dJ}{dk}-\left(\frac{\hat{\gamma}}{\rho}\right)^2\left(\Delta^2+\frac{1}{k^2}\right)J=0, \qquad (8)$$

where $\hat{\gamma}=\gamma\tau_A$, $\Delta^2=d^2(1+\nu_{ei}/2\gamma)$ and $d\equiv d_e/r_s$. Equation (8) is subject to the following boundary conditions (Pegoraro and Schep, 1986). J must vanish for $|k|\rightarrow\infty$ in order for the current density in x space to be regular. For small values of k, J must behave as $J\sim 1-(\hat{\gamma}^2k^2/2)+(\hat{\gamma}^2\lambda_H|k|^3/3)+0(k^4)$. Here, the first two contributions permit matching to a constant radial displacement in the outer MHD region. The last contribution arises from the matching to the x^{-1} correction to the displacement approaching the singular layer from outside. It involves the ideal MHD parameter, $\lambda_H\propto-\delta\hat{W}\sim(r_s/R)^2(\beta^2_p-\beta^2_{p,MHD})$, with $\delta\hat{W}$ the potential energy functional, $\beta_p=-[8\pi/B^2_p(r_s)]\int_0^{r_s}(dp/dr)r^2dr$ a poloidal beta parameter which depends on the average pressure gradient within the q = 1 surface and $\beta_{p,MHD}\leq 0.3$ a critical toroidal MHD threshold value (Bussac et al, 1975). The normalization is chosen so that, for $\delta\hat{W}<0$, the ideal MHD growth rate and layer width are $\gamma_{MHD}\tau_A\approx\delta_{MHD}/r_s\approx\lambda_H$.

In solving Eq. (8), first we consider briefly the small Larmor radius limit, $\rho_i\sim\rho_s<\delta r_s$. Thus we can approximate $L\sim(\rho k)^2$ and neglect $\Gamma\tau$ as compared to L^{-1}. Equation (8) can then be solved in terms of confluent hypergeometric functions. Using the boundary conditions at small $|k|$, we obtain the dispersion relation

$$\hat{\gamma}=\lambda_H(Q/4)^{3/2}\Gamma[(Q-1)/4]/\Gamma[(Q+5)/4], \qquad (9)$$

where $Q=\hat{\gamma}/\Delta$ and $\Gamma(z)$ is the gamma function. In the interesting limit $|\lambda_H|<\Delta$, Eq. (9) yields

$$\gamma\tau_A\approx(d_e/r_s)(1+\nu_{ei}/2\gamma)^{1/2}. \qquad (10)$$

The eigenfunction is $J(k)\approx\exp(-\Delta^2k^2/2)$. When $\nu_{ei}>>\gamma$, Eq. (10) gives the well known resistive internal kink growth rate, $\gamma\tau_A\approx\varepsilon_\eta^{1/3}$, where $\varepsilon_\eta=(d^2\nu_{ei}\tau_A/2)\propto\eta$ is the inverse of the magnetic Reynolds' number (Coppi et al, 1976). In the collisionless limit, one obtains $\gamma\tau_A\approx d_e/r_s$.

Next we consider the more realistic limit $\rho_i>d_e$. Equation (8) can be solved analytically by adopting a Padé approximation of the ion response function,

$$L^{-1} \approx 1 + (\rho k)^{-2}, \tag{11}$$

which is an interpolation formula between the fluid and the large Larmor radius responses. With this approximation, multiplying Eq. (8) by ρ^2, and using the isothermal electron equation of state ($\Gamma = 1$), we find that ρ_i and ρ_s combine into a single scale length,

$$\rho_\tau = (\rho_i^2 + \rho_s^2)^{1/2} = (1 + \tau)^{1/2}\, \rho_i. \tag{12}$$

The implication is that the equation for J remains unchanged in the cold ion limit $T_i \to 0$ and $\rho_\tau \to \rho_s$. Thus we can anticipate that a result correct in the ion kinetic regime can be recovered simply replacing ρ_s by ρ_τ in the dispersion relation obtained by Hazeltine and Strauss (1978) and by Drake (1978). A similar conclusion was reached by Aydemir (1991), who employed a four-field fluid model to analyse the stability of m=1 modes, and by Zakharov and Rogers (1992b), who used the two-fluid Braginskii model. We point out, however, that the electrostatic potential is significantly different in the cold and kinetic ion regimes, as will be shown below. In addition, the Padé approximation is not entirely correct if diamagnetic effects are included in the ion response function. Then, only the kinetic description can fully account for the proper ion equation of state (Pegoraro et al, 1988).

The resulting dispersion equation can be solved by a double asymptotic matching technique. We identify two overlapping intervals in k, $(\Delta k)^2 < 1$ and $(\hat{\rho} k)^2 > 1$, where $\hat{\rho} \equiv \rho_\tau / r_s$, corresponding in x space to an inner sublayer of width $\delta_{inner} \sim d$, where electron inertia is important, nested into a broader layer of width $\delta \sim \hat{\rho}$. For $(\Delta k)^2 < 1$, Eq. (8) reduces to

$$(d/dk)\,[(\hat{\rho}^2 + k^{-2})\, dJ/dk] - (\hat{\gamma}/k)^2\, J = 0. \tag{13}$$

This can be solved exactly in terms of a combination of hypergeometric functions of $-(\hat{\rho} k)^2$, with the constants of integration fixed by the boundary condition at small k. For $(\hat{\rho} k)^2 > 1$, Eq. (8) reduces to

$$d^2J/dk^2 - (\hat{\gamma}/\hat{\rho})^2\, (\Delta^2 + k^{-2})\, J = 0. \tag{14}$$

The solution of this equation that behaves well at $|k| \to \infty$ is $J = C\, (\sigma |k|)^{1/2}\, K_\nu(\sigma |k|)$, where $\sigma = \hat{\gamma}\Delta/\hat{\rho}$, $\nu^2 = (1/4) + (\hat{\gamma}/\hat{\rho})^2$ and $K_\nu(z)$ is a modified Bessel function of the second type. Matching the two solutions in the interval

$\hat{\rho}^{-1} > k > \sigma^{-1}$ determines the constant C and leads to the eigenvalue condition. In particular, in the relevant limit $\hat{\rho} > \hat{\gamma} > \nu_{ei}\tau_A$, the dispersion relation reduces to

$$(\pi/2)\hat{\gamma}^2 = \hat{\rho}\lambda_H + \hat{\rho}^2 d/\hat{\gamma}. \qquad (15)$$

Near ideal MHD marginal stability, i.e. for $|\lambda_H| < \hat{\rho}^{1/3}d^{2/3}$, we obtain the growth rate

$$\gamma\tau_A \approx (2/\pi)^{1/3} d^{1/3}\hat{\rho}^{2/3} \equiv \gamma_o\tau_A, \qquad (16)$$

which is higher than the growth rate in (10). A modest enhancement of the growth rate (16), by a factor $(1+\nu_{ei}/2\gamma_o)^{1/6}$, is found for $\nu_{ei} \leq \gamma_o$.

For $(\hat{\rho}d^2)^{1/3} < \lambda_H < \hat{\rho}$, the growth rate (Pegoraro et al, 1988) $\hat{\gamma} \sim (\lambda_H\hat{\rho})^{1/2}$ is obtained from (15). The ideal MHD result, $\hat{\gamma} \approx \lambda_H$, applies to the limit $\lambda_H > \hat{\rho}$, where Eq. (15) is no longer valid. In the limit $\lambda_H < -(\hat{\rho}d^2)^{1/3}$, Eq. (15) yields $\hat{\gamma} \sim \hat{\rho}d/|\lambda_H|$, so that, for sufficiently large and negative λ_H, γ drops below ν_{ei} and the (semi) collisional regime is recovered. A graph of γ/γ_o versus $\lambda_H/\rho^{1/3}d^{2/3}$ is shown in Fig. 1. The instability drive increases with λ_H. For $\lambda_H > 0$, the source of excitation energy is related to the ideal MHD potential energy, $-\delta W$, to which λ_H is proportional. On the MHD stable side of the spectrum, the instability is driven by the magnetic energy released during reconnection, a measure of which is given by $\Delta' \approx -\pi/\lambda_H$ (Ara et al, 1978), with Δ' the familiar parameter of tearing mode theories.

Examples of the perturbed parallel current density and electrostatic potential across the reconnection layer for $\lambda_H = 0$ and $\rho_\tau/d_e = 5$ are shown in Fig. 2. The larger part of $J_{||}(x)$ is localized over a distance $x \sim d_e$, where the decoupling of the electrons from the magnetic field lines can occur, with a tail extending up to distances $x \sim \rho_\tau$. This profile remains unchanged in the cold ion limit $T_i \to 0$ keeping ρ_s fixed ($T_e \to 2T_e$). On the other hand, the profile of $\phi(x)$ is very different in the cold and kinetic ion limits, as can be inferred by inspection of Eq. (5). For kinetic ions ($T_i \sim T_e$), $\phi(x)$ is rapidly varying up to distances $x \sim d_e$, while it approaches a constant over distances $x \sim \rho_\tau$. This behaviour reflects the decoupling of the electron and ion radial flows at

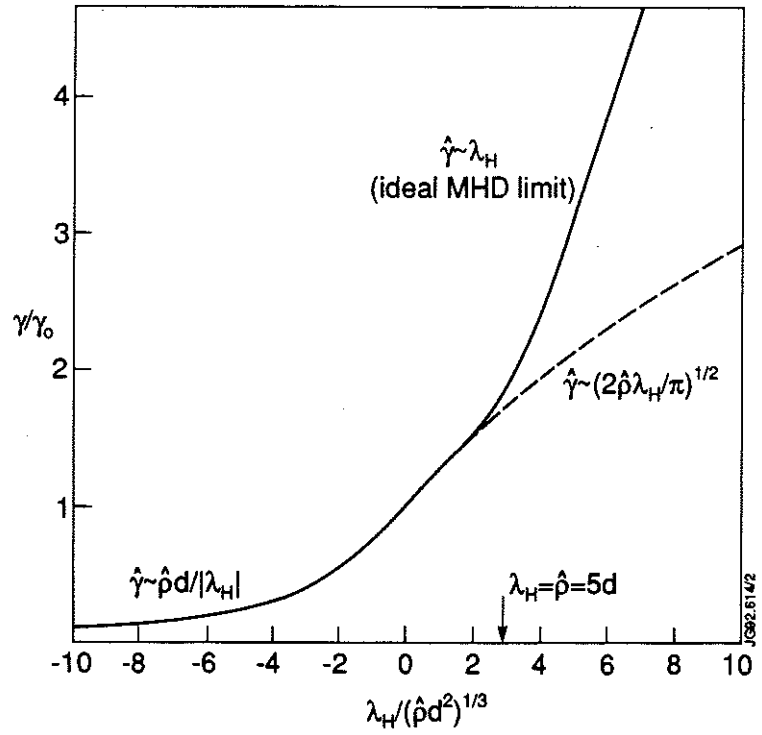

Figure 1. Graph of normalized growth rate, γ/γ_o, versus $\lambda_H/\hat{\rho}^{1/3}\,d^{2/3}$. The portion of the solid curve for $\lambda_H > \hat{\rho}$, where we have chosen $\hat{\rho}/d = 5$, corresponds to the ideal MHD limit $\hat{\gamma} \approx \lambda_H$, with $\hat{\gamma} \equiv \gamma\tau_A$. The dashed curve and the remaining part of the solid curve correspond to the solution of Eq. (15).

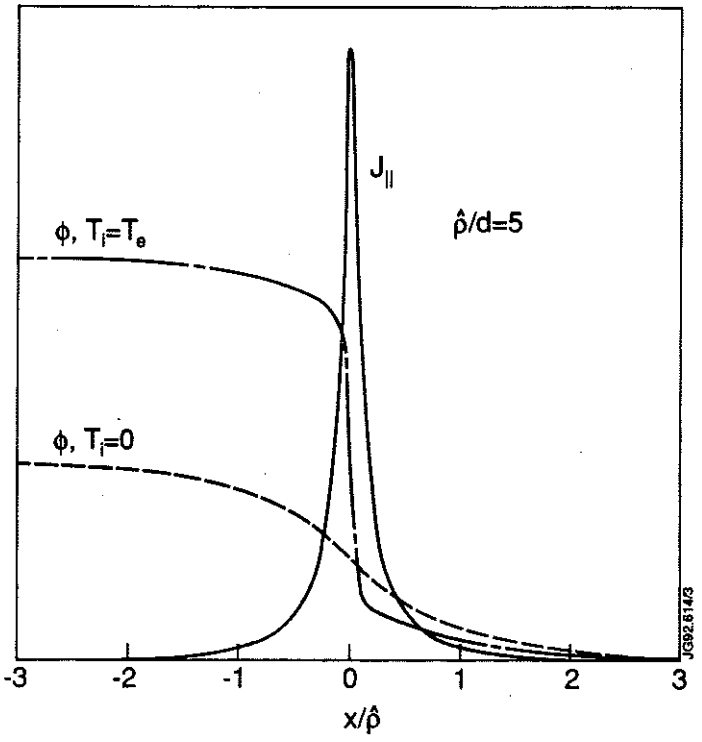

Figure 2. Graph of the current density $J_{||}$, and of the electrostatic potential, ϕ, for two values of T_i/T_e, versus the normalized distance from the q = 1 surface, $x/\hat{\rho}$.

distances $x < \rho_i$. By contrast, for fluid ions ($T_i/T_e \to 0$), the structure around $x \sim d_e$ disappears and $\phi(x)$ varies more gently over the scale length ρ_s.

These results are valid as long as diamagnetic effects can be neglected. These effects have been considered by Porcelli (1991) following the earlier analysis of semi-collisional m = 1 modes by Pegoraro et al (1988). Here, we report only the main findings. Using a Padé approximant for the ion response function, the modified dispersion relation at ideal MHD marginal stability ($\lambda_H = 0$) is

$$(\gamma + i\omega_{*e})\,(\gamma + i\omega_{*i})^{2/3}\,(\gamma + i\omega_{di})^{1/3} = \gamma_o^2, \tag{17}$$

where $\omega_{*e} = (cT_e / eBr_s)(d\ell nn_e / d\ell nr)$, $\tau\omega_{*i} = -\omega_{*e}$, $\omega_{di} = (1 + \eta_i)\,\omega_{*i}$ and $\eta_i = d\ell n\, T_i / d\ell n\, n$. Then, assuming $\tau \sim 1$, stabilization is predicted when

$$\frac{\omega_{*i}}{\gamma_o} = \frac{1}{2}\left(\frac{\pi}{1+\tau}\right)^{1/3}\left(\frac{m_i}{m_e}\right)^{1/6}\left(\frac{L_s}{r_n}\right)\beta_i^{2/3} > 1. \tag{18}$$

For nonzero values of λ_H we may conclude that a threshold in λ_H exists corresponding to the criterion $\gamma(\lambda_H) \sim \omega_*$, with $\gamma(\lambda_H)$ the solution of (15). This criterion is more easily satisfied for negative λ_H where γ drops below γ_o. However, as we remarked earlier, the Padé approximant for the ion response is not entirely correct when $\gamma \sim \omega_*$ and η_i becomes large. For instance, Pegoraro et al (1988), using the full kinetic ion response, found a residual growth rate for values of $\eta_i > \eta_{i,cr} \sim 1.6$.

We check the consistency of the obtained results, in particular of Eq. (16), with the assumed isothermal electron equation of state. The current density is localised in Fourier space over a distance $k \leq \sigma^{-1} \approx d^{-1}\,(d/\hat{\rho})^{1/3}$. In co-ordinate space, this corresponds to values of $x \geq (\hat{\rho}/d)^{1/3}\,d$. The latter inequality is equivalent to $\gamma_o^2 \leq k_\parallel^2 v_{the}^2$, where the isothermal condition applies. In particular, having assumed $d < \hat{\rho}$, the solutions of Eqs. (13) and (14) can be matched entirely in the isothermal domain $\hat{\rho}^{-1} < k < \sigma^{-1}$. Finite thermal conductivity alters the rate of decay of the eigenfunction at large $k > \sigma^{-1}$, but the eigenvalue condition is not affected to leading order in the small parameter $d/\hat{\rho}$. This conclusion is supported by the analysis of Berk et al (1991) and of

Coppi and Detragiache (1992), who have obtained similar results with a kinetic electron model which has a more proper representation of the electron equation of state.

The main conclusion of the linear analysis is that m = 1 magnetic reconnection can remain a very fast process at high temperatures, contrary to expectations based on collisional models. In Fig. 3 we present a sketch of γ vs $T \equiv T_e = T_i$ for near ideal MHD marginal stability conditions ($\lambda_H \to 0$), keeping all other parameters constant. At low temperatures, the resistive internal kink mode is found with a growth rate $\gamma \propto T^{-1/2}$ (Coppi et al, 1976). At intermediate temperatures, corresponding to $\left(\hat{\rho}/\varepsilon_\eta^{1/3}\right)^{2/7} d < \varepsilon_\eta^{1/3} < \hat{\rho}$, one finds the semi-collisional growth rate $\hat{\gamma} \approx (2/\pi)^{2/7} \hat{\rho}^{4/7} \varepsilon_\eta^{1/7} \propto T^{1/14}$ (Pegoraro et al, 1988), which is virtually independent of the temperature. At higher temperatures, the collisionless growth rate (16) increases with temperature as $\gamma \propto T^{1/3}$. In this regime the condition for diamagnetic stabilization at $\lambda_H = 0$

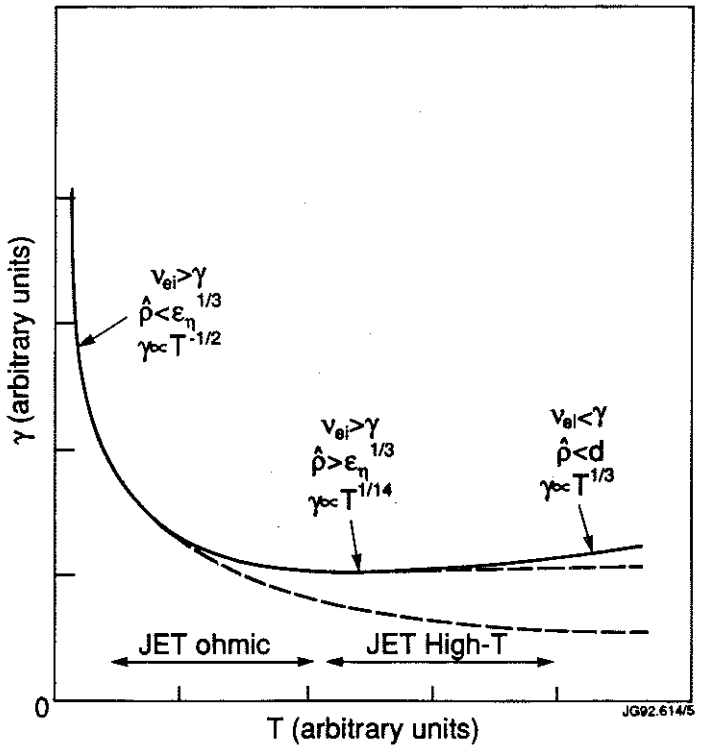

Figure 3. Scalings of the growth rate, γ, with temperature, T, for $\omega_* = 0$ and all other parameters held constant, spanning the collisional (low-T), semi-collisional (intermediate-T) and collisionless (high-T) regimes.

involves the plasma β parameter [cf. Eq. (18)]. This condition is more stringent than predicted by the two-fluid model. The stabilization condition $\omega_* > \gamma$ is more easily met for values of $\lambda_H < -\hat{\rho}^{1/3} d^{2/3}$ where γ drops below γ_0.

III. NONLINEAR CONSIDERATIONS

The nonlinear evolution of the m = 1 mode in the collisionless regime has not yet been clarified. The purpose of this Section is to point out some of the subtleties involved in the problem.

We consider the early nonlinear evolution of an unstable m = 1 mode, up to radial displacements that are large compared with the linear layer width but small compared with the q = 1 radius. Under these conditions the toroidal coupling of the m = 1 component with poloidal harmonics having a different helicity remains weak, so that the cylindrical approximation should be adequate.

At first, one may consider the limit $\rho_s \sim \rho_i \to 0$ and neglect diamagnetic effects. Although not entirely consistent with the experimental parameters, this limit leads to a much simplified problem. On one hand, fluid ions may be considered, on the other hand, the relevant Ohm's law reduces to

$$\vec{E} + \frac{1}{c}\vec{V} \times \vec{B} = \eta \vec{J} + \left(m_e / ne^2\right) d\vec{J} / dt. \tag{19}$$

Furthermore, it may be assumed that the nonlinear evolution is in agreement with the Sweet-Parker scenario (Sweet, 1958; Parker, 1957), as hypothesized by Kadomtsev (1975). The Kadomtsev model has been confirmed by several resistive MHD numerical simulations of m = 1 island growth. Thus, one may look for the modification of Kadomtsev's scaling for m = 1 magnetic reconnection in the weakly collisional regime where the second term at the r.h.s. of Eq. (19) dominates over the first (Wesson, 1990).

While Kadomtsev's description of the m = 1 reconnection process appears qualitative in places, a recent contribution by Waelbroeck (1989) is seen to provide a sound analytical basis for the Kadomtsev process. In Waelbroeck's

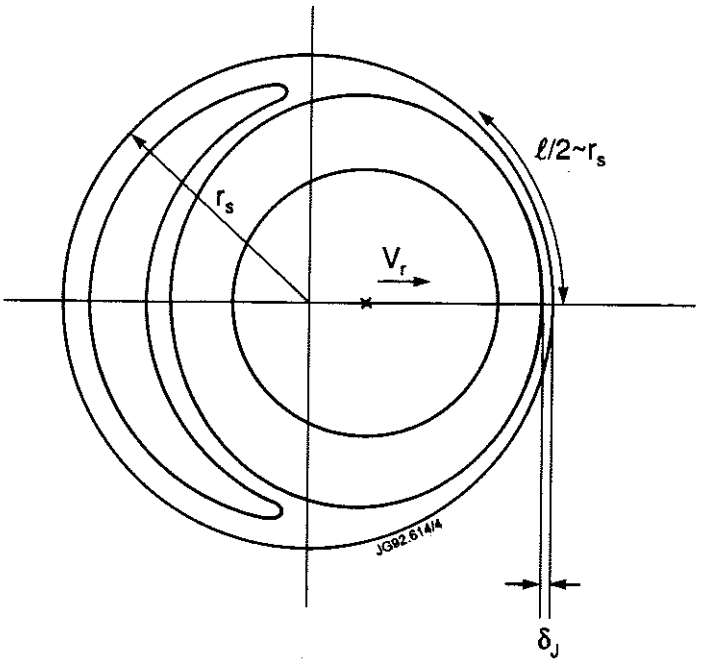

Figure 4. Contour levels of the poloidal flux function, ψ, showing the ribbon-like structure of the reconnection region according to Sweet-Parker's and Waelbroeck's scenario.

work, it is shown that an ideal helical "quasi-equilibrium" with a magnetic island is formed, whose basic geometry is shown in Fig. 4. This analytic solution exhibits a current sheet. The island separatrix does not have an X-point, as usual, but a singular line of length ℓ corresponding to the length of the current sheet. Thus, reconnection takes place within a singular, ribbon-like layer of width δ_J and length ℓ. The important feature is that the length $\ell \sim r_s$ is independent of the rate of current diffusion within the ribbon, as in the Sweet-Parker and Kadomtsev models.

The relevance of Waelbroeck's quasi-equilibrium assumption relies on the inequalities $\tau_A^* << \tau << \tau_\eta^*$, where τ_A^* is the characteristic Alfvén time of the helical equilibrium, τ is the reconnection time scale and τ_η^* is the diffusion time of the current sheet. Now, $\tau_\eta^* \propto \delta_J^2$. For instance, for resistive Sweet-Parker evolution, $\delta_J \propto \eta^{1/2}$, so that τ_η^* becomes independent of resistivity and the inequality $\tau_A^* << \tau_\eta^*$ relies on geometrical and beta factors. Baty et al (1991) have recently pointed out that the formation of a current sheet is not always

observed in numerical simulations of the nonlinear m = 1 mode evolution. When it is not, their interpretation is the breakdown of the inequality $\tau_A^* << \tau_\eta^*$. Thus m = 1 reconnection processes which do not obey the basic Sweet-Parker geometrical configuration in Fig. 4 may be possible.

In the following, we shall assume that the plasma parameters are such to satisfy the requirements for the validity of Waelbroeck's solution, i.e. we shall adopt the geometry of Fig. 4 Then, the following arguments lead to an estimate of the reconnection time. Mass conservation implies

$$V_r/\delta_f \sim V_\vartheta/\ell. \tag{20}$$

where δ_f is the width of the radial ion flow and $\ell \sim r_s$ as in Fig. 4. In the limit $\rho_i \sim \rho_s \to 0$, there is only one characteristic width of the reconnection region and we can set $\delta_f \sim \delta_J$. The poloidal flow V_ϑ is determined by energy conservation. The work done by the pressure gradient in the poloidal direction on a unit volume of the plasma is of the order of the magnetic pressure of the helical field $B_*=(1-q)B_\vartheta$ evaluated at the edge of the reconnection layer, i.e. $\Delta p \sim B^2_{*edge}/8\pi$, with $B_{*edge} = B_*(x + \xi_o/2) \sim -q'(r_s)\xi_o B_\vartheta/2$ and ξ_o the radial plasma displacement outside the layer. This work results in an increase of the kinetic energy of the poloidal flow, i.e. $\Delta p \sim m_i n_i V_\vartheta^2/2$, leading to

$$V_\vartheta \sim \xi_o/\tau_A. \tag{21}$$

Now, ξ_o is a function of time. Using $v_r = d\xi_o/dt$ and inserting this and Eq. (21) back into Eq. (20), we obtain an evolution equation for $\xi_o(t)$:

$$\tau_A \, d\xi_o / dt = (\delta_f / r_s)\ c_o \xi_o \tag{22}$$

where c_o is a numerical factor of order unity which can be determined on the basis of Waelbroeck's quasi-equilibrium (Zakharov and Rogers, 1992a).

From Eq. (22) one observes that, if δ_f is constant as a function of time, the early nonlinear evolution of $\xi_o(t)$ is characterized by exponential growth. For the classic (resistive) Sweet-Parker problem, $\delta_f \sim \delta_J = \delta_J(t)$ shrinks in time and the evolution of $\xi_o(t)$ is slower. To show this, we estimate the scale length δ_J from Ohm's law (19). In the resistive limit, the $\vec{V}x\vec{B}$ term balances the $\eta\vec{J}$ term. Taking the helical component, we find $V_r B_* \sim \eta c J_h \sim \left(\eta c^2 / 4\pi\right) B_* / \delta_J$,

the latter relation corresponding to Ampère's law. Therefore, $\delta_J \sim \left(r_s^2 / \tau_\eta\right)\left(d\xi_o / dt\right)^{-1}$, where $\tau_\eta^{-1} = \eta c^2 / 4\pi r_s^2$. Substituting $\delta_J \sim \delta_f$ in Eq. (22), we obtain simple algebraic growth,

$$\xi_o(t) / r_s \sim \left(t / \tau_K\right)^2 \tag{23}$$

where $\tau_K \equiv \left(\tau_A \tau_\eta\right)^{1/2}$ is Kadomtsev's reconnection time. The width of the current channel scales as $\delta_J / r_s \sim \left(r_s / \xi_o\right)^{1/2}\left(\tau_A \tau_\eta\right)^{1/2} \propto \eta^{1/2}$.

One may attempt to repeat the same argument in the collisionless limit, where the $\vec{V}\times\vec{B}$ term in Ohm's (19) is balanced by the inertial term. Wesson (1990) estimated

$$V_r B_* \sim \left(m_e c / ne^2\right) V_r \ \partial J_h / \partial r \sim \left(d_e / \delta_J\right)^2 V_r B_* \tag{24}$$

which implies that $\delta_J \sim d_e$. Note that this estimate for δ_J is the same as the collisionless linear layer width [in the limit $\rho_i \sim \rho_s \to 0$, see below Eq. (10)], and that δ_J is constant in time. Then, from Eq. (22) one finds that the radial displacement continues to grow exponentially into the nonlinear phase at approximately the linear growth rate, i.e. $\xi_o(t) = \xi_o(0)\ \exp\left[c_1(d_e/r_1)(t/\tau_A)\right]$, with c_1 a numerical factor of order unity (exponential growth was not predicted by Wesson, as the evolution equation (22) for ξ_o was not derived explicitly).

Things, however, are not that simple, as numerical simulations by Drake and Kleva (1991) revealed a behaviour that differs from that implied by Eq. (24). As shown in Fig. 2 of Drake and Kleva's paper, the width δ_J of the collisionless current channel collapses rapidly well below the skin depth, bringing the reconnection process to a virtual halt. Physically, the impedance to the induced parallel electric field is provided by electrons transiting through the reconnection region. However, the X-line is a stagnation line of the flow. Therefore, electrons very close to the X-line remain in the acceleration region for a long time, acquiring very large parallel speeds. The result is that most of the current is carried by these electrons in a highly localised layer.

Going back with hindsight to Wesson's estimate, Eq. (24), it is clear that the most delicate step is balancing the electric field with the inertial term $\left(m_e / ne^2\right)\vec{V}_e \cdot \nabla\vec{J}$. This balance must fail at the X-line where the reconnection

sheet has its maximum so that $V_r \partial J_{\|} / \partial r = 0$. The term $\partial J_{\|} / \partial t$ takes over the term $\vec{V}_e \cdot \nabla \vec{J}$ in a subsidiary layer with a time-dependent width narrower than the skin depth. Wesson himself was aware of the problem and indicated the need for further elaboration (Wesson, 1990).

It is highly unlikely that such a narrow current sheet with a scale size much smaller than the skin depth can survive in a real plasma. Thus Drake and Kleva (1991) went on to propose that the electron current layer becomes unstable to a current convective instability. The resulting anomalous current diffusion allows reconnection to proceed.

There is, however, another possible way out. If finite values of ρ_τ are considered, the actual nonlinear behaviour may again differ from that observed by Drake and Kleva. Indeed, it is plausible that the width δ_f of the ion radial flow does not become narrower than ρ_τ. The crucial point, however, is whether the current density profile is significantly affected by consideration of the kinetic ion response and/or of the parallel electron pressure gradient. In fact, the ultimate region where the decoupling between the plasma and the magnetic field can take place is where the electron inertia is important, i.e. the region corresponding to the width of the current channel, δ_J. Preliminary indications (Kleva et al, 1992) are that $\delta_f \sim \rho_\tau > \delta_J$. Then, considering Eq. (22), we reckon two possibilities. If the reasoning leading to Eq. (22) is correct, than this equation with $\delta_f \sim \rho_\tau$ predicts experimental growth at the nonlinear rate $\gamma_{NL} \tau_A \sim \rho_\tau / r_s$ (Zakharov and Rogers, 1992a). Since this result does not depend explicitly on the electron inertia, it applies also to the limit $d_e \to 0$. It appears that reconnection would be inessential in this case, and that an internal m=1 kink mode would continue to grow thanks to the parallel electron pressure gradient, in contrast with the analysis of Rosenbluth et al (1973) who predicted nonlinear saturation in the ideal MHD limit. The second possibility is that either the basic reconnection geometry of Fig. 4 or the force balance relation (21) is incorrect in the large ρ_τ limit. Indeed, if $T_i \sim T_e$, a more complex kinetic relation should replace the fluid argument leading to Eq. (21). On the other hand, if $T_i << T_e$, the ion pressure cannot be used to determine

the ion poloidal flow as given by Eq. (21). Thus, for any T_i, Eq. (22) may have to be modified. Work is in progress to clarify these aspects.

IV EXPERIMENTAL EVIDENCE AND CONCLUSIONS

It is premature to present a detailed comparison between theory and the experimental evidence of the sawtooth collapse in high temperature regimes. Nevertheless, it useful to discuss the relevant experimental features that the present model may attempt to address.

There are several different kinds of sawtooth relaxations, a fact which, by itself, poses a challenge to theoretical predictions. There is, however, a pattern observed in high temperature JET discharges with auxiliary ICRF heating, as exemplified by Fig. 5 (Edwards, 1991). The insert in Fig. 5 shows the relaxation of the soft X-ray line-integrated emissivity, $I_X(t)$, as viewed from a chord passing near the location of the equilibrium magnetic axis. The sudden drop of I_X reflects corresponding drops in the electron temperature and density as observed along this chord. It is important to realize that, initially, this drop is

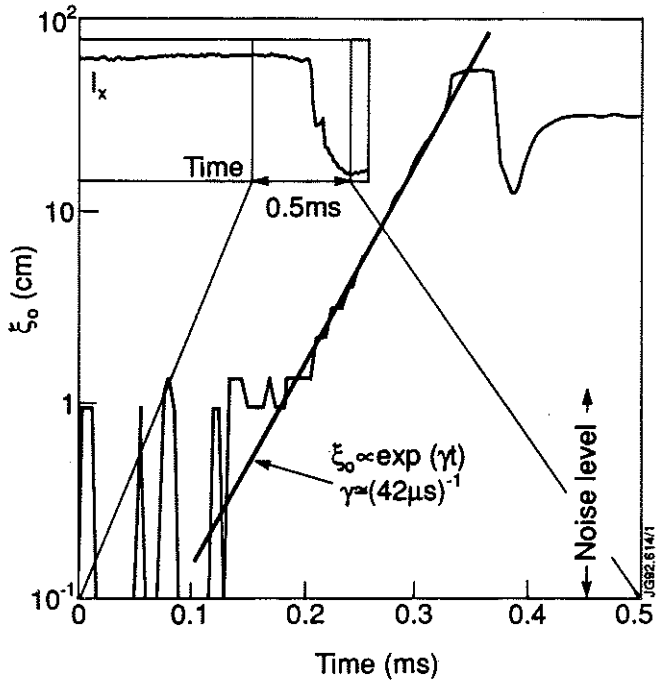

Figure 5. Graph of the displacement, ξ_o, of the peak of the soft X-ray emissivity profile versus time during the interval indicated in the small frame. I_X is the line-integrated emissivity along a central chord. The data correspond to a relaxation terminating a prolonged sawtooth-free period in the presence of ICRF heating at JET (courtesy of A.W. Edwards).

to be attributed to a shift of the peak values of T_e and n_e out of the line of sight. In fact, two phases of the sawtooth relaxation can be identified. The first phase, which we refer to as the "displacement phase", is characterized by a displacement of the soft X-ray emissivity profile, whose peak is believed to coincide with the original magnetic axis. As shown in Fig. 5, this axis moves exponentially in time from its equilibrium position to a final position, r_{max}, which, in the example shown, is roughly 80% of the sawtooth inversion radius. The peak value of the emissivity profile is nearly constant during this phase. One prominent feature in this example is the sudden onset of the instability, which is seen to come out of the noise level ($\xi_o \sim$ 1cm) with a fast growth rate in the order of $\gamma_{exp}^{-1} \sim$ 40-50μs. More generally, the displacement phase has a duration in the range $\tau_{disp} \sim$ 100-300μs, and the ratio of r_{max} to the noise level corresponds roughly to three e-folding times (i.e. $\gamma_{exp}^{-1} \sim \tau_{disp}/3$). This is followed by a second phase, which we refer to as the "diffusion phase", where the peak of the X-ray emissivity profile drops on a time scale, τ_{diff}, which can vary greatly between 100μs to several ms. The two phases sometimes overlap. Contrary to Kadomtsev's original prediction (Kadomtsev, 1975), the on-axis value of the q parameter in the relaxed state, after toroidal symmetry has been restored, is believed to remain below unity (O'Rourke, 1991). Also, there is some evidence that the magnetic axis of the relaxed equilibrium is the same as the original axis before the onset of the instability.

In the example shown in Fig. 5, the sawtooth relaxation follows a prolonged stable period where m=1 modes are believed to have been stabilized by the high energy ions produced by ICRF heating. Following, for instance, Porcelli (1991), fast ion effects can be included in the present model through their contribution to the potential energy functional δW, i.e. through an appropriate modification of the parameter λ_H. During the sawtooth free period, as the q=1 radius expands, the modified λ_H is believed to evolve from large negative values, where the m=1 mode is stable with the help of diamagnetic effects, to values $\lambda_H \gtrsim -\hat{\rho}^{1/3} d^{2/3}$ where diamagnetic stabilization is no longer effective. It has been argued that the sudden onset of the sawtooth

relaxation poses a challenge to linear stability models (Wesson et al, 1991). Here, we conjecture that, as λ_H increases and crosses a diamagnetic threshold, an m=1 magnetic island may at first grow very slowly until it reaches a width, W_{crit}, where diamagnetic effects are removed because of local quasilinear flattening of the equilibrium density and temperature profiles. Thus for $W \geq W_{crit}$, the m=1 growth rate may rapidly attain the value, $\gamma \sim \gamma_o$, that is found in the present analysis setting $\omega_* = 0$. A value $W_{crit} \sim 1$cm would then explain the behaviour illustrated in Fig. 5.

With the above conjecture, the model presented in this paper may address the time scale and evolution of ξ_o during the displacement phase. In the absence of conclusive theoretical indications on the nonlinear mode evolution, we may compare the linear growth rate γ_o given by Eq. (16) with the experimental growth rate γ_{exp}. Typical reference parameters of JET discharges of the type shown in Fig. 5 are $R \approx 3$m, $r_s \approx 0.4$m, $B \approx 3$T, $n_e(r_s) \approx 3 \times 10^{19}$ m^{-3}, $T_e(r_s) \approx 5$ KeV and $Z_{eff} \approx 2$. With these parameters, the electron-ion collision time is $\tau_{ei} \approx 130$ μs. Thus, $\nu_{ei} = \tau_{ei}^{-1}$ is one to four times smaller than γ_{exp}. The plasma skin depth is $d_e \approx 1$mm. Considering a deuterium plasma with $T_i(r_s) \approx T_e(r_s)$, we find an ion Larmor radius $\rho_i \approx 0.34$cm. Assuming a local magnetic shear value $s(r_s) \approx 0.6$, the growth rate in Eq. (16) is $\gamma_o^{-1} \approx 86$μs, which falls in the middle of the experimental range of values of γ_{exp}^{-1}. Finally, $\beta_i(r_s) \approx 0.67\%$ and, assuming $L_n \sim 1$m, we find $\omega_{*i}/\gamma_o \approx 0.4$.

During the second stage of the sawtooth relaxation, it can be expected that the toroidal coupling of the m=1 poloidal component with harmonics having a different helicity becomes important. In this case, magnetic field lines would ergodically fill regions of space, initially near the island separatrix, thus affecting the width of the reconnection layer. Also, for a sufficiently wide ergodic region, the radial heat transport may be enhanced significantly, leading to a decoupling of the contour levels of plasma temperature (and X-ray emissivity) from those of equal magnetic flux (Baty et al, 1992). This circumstance may allow for a relaxed state with flattened temperature and density profiles but with q remaining below unity on axis. Clearly, the

cylindrical model presented here cannot address this second phase of the relaxation process.

In summary, the main conclusion we can draw at this point is that m=1 magnetic reconnection can remain a virulent process at high temperature, contrary to expectation based on collisional models. In the limit $\nu_{ei} < \gamma$ and $\rho_\tau > d_e$, the linear growth rate $\gamma_o / \omega_A \approx (2/\pi)^{1/3} (d_e / r_s)^{1/3} (\rho_\tau / r_s)^{2/3}$ depends on the plasma skin depth, $d_e = c/\omega_{pe}$, on the ion Larmor radius, $\rho_i = v_{thi} / \Omega_{ci}$ and on the ion sound Larmor radius, $\rho_s = c_s / \Omega_{ci}$, with $c_s = (T_e/m_i)^{1/2}$, the latter two scale length combining into the hybrid Larmor radius, $\rho_\tau = \left(\rho_i^2 + \rho_s^2\right)^{1/2}$. The scale-length ρ_s is introduced by the electron pressure gradient force in Ohm's law. For typical high temperature JET parameters, $\gamma_o^{-1} \sim 50-100\mu s$, which compares favourably with the observed instability growth time of internal plasma relaxations. On the basis of Eq. (18), the condition for diamagnetic stabilization at $-\lambda_H \propto \delta W = \delta W_{MHD} + \delta W_{hot} = 0$ (with δW_{hot} the contribution of the high energy ions) does not improve with temperature at fixed $\beta_i = 8\pi p_i / B^2$. The stabilization criterion is more easily met for positive δW, corresponding to $\lambda_H \lesssim -\hat{\rho}^{1/3} d^{2/3}$, where γ drops below γ_o. The nonlinear m=1 mode evolution has not yet been clarified. Indications are that the scale-length ρ_τ may play an essential role in the nonlinear stage, where it limits the width of the ion flow channel.

ACKNOWLEDGEMENTS

The author would like to acknowledge F. Pegoraro and T.J. Schep for their collaboration on ion kinetic effects, A. W. Edwards for discussions on the experimental evidence and for kindly providing Fig. 5, B. Rogers, F. L. Waelbroeck and J.A. Wesson for discussions on the nonlinear mode evolution.

REFERENCES

Antonsen, T. M., Jr., and B. Coppi (1981). Phys. Rev. Lett. A81, 335.

Ara, G. et al. (1978). Ann. Phys. 112, 443.

Aydemir, A.Y. (1991). Phys. Fluids B3, 3025.

Aydemir, A.Y. (1992). IFS Report IFSR#560.

Basu, B. and B. Coppi (1981). Phys. Fluids 24, 465.

Baty, H., J.-F. Luciani and M.N. Bussac (1991). Nuclear Fusion 31, 2055.

Baty, H., J.-F. Luciani and M. N. Bussac (1992). Nuclear Fusion 32, 1217.

Berk, H.L., S.M. Mahajan and Y.Z. Zhang (1991). Phys. Fluids B3, 351.

Bussac, M.N., R. Pellat, D. Edery and S. Soulé (1989). Phys. Rev. Lett. 35, 1638.

Coppi B. and P. Detragiache (1992). Phys. Lett. A168, 59.

Coppi M.N., R. Galvão, R. Pellat, M.N. Rosenbluth and P.H. Rutherford (1976), Fiz. Plazmy 2, 961 [Sov. J. Plasma Physics 2, 533].

Drake, J. F. (1978). Phys. Fluids 21, 1777.

Drake, J. F. and R. G. Kleva (1991). Phys. Rev. Lett. 66, 1458.

Edwards, A.W. (1991). Private communication.

Edwards, A.W. et al. (1986). Phys. Rev. Lett. 57, 210.

von Goeler, S., W. Stodiek and N. Sauthoff (1974). Phys. Rev. Lett. 33, 1201.

Hazeltine, R. D. and H. R. Strauss (1978). Phys. Fluids 21, 1007.

Kadomtsev, B.B. (1975). Fiz. Plazmy 1, 710 [Sov. J. Plasma Phys. 1, 389].

Kleva, R.G., J.F. Drake and F.L. Waelbroeck (1992). Sherwood Theory Meeting, Santa Fe, N.M., paper 2C16.

McGuire, K. et al. (1986). Phys. Fluids 2, 1287.

Mikhailovskii, A.B. (1974), Theory of Plasma Instabilities (Consultant Bureau, New York, 1974), Vol. 2.

O'Rourke, J.J. (1991). Plasma Phys. Contr. Fusion 30, 1475.

Parker, E.N. (1957). J. Geophys. Research 62, 509.

Pegoraro, F. and T. J. Schep (1986). Plasma Phys. Contr. Fusion 28, 647.

Pegoraro, F., F. Porcelli and T.J. Schep (1989). Phys. Fluids B1, 364.

Porcelli, F. (1991). Phys. Rev. Lett. 66,425.

Porcelli, F. (1991). Plasma Phys. Contr. Fus. 33, 1601.

Rosenbluth, M.N., R.Y., Dagazian and P.H. Rutherford (1973). Phys. Fluids 61, 1984.

Sweet, P.A. (1958). Electromagnetic Phenomena in Cosmic Physics, ed. B. Lehnert (Cambridge University Press), p.123.

Vasyliunas, V.M. (1975). Rev. Geophs. Space Phys. 13, 303.

Waelbroeck, F.L. (1989). Phys. Fluid B1, 2372.

Wesson, J.A. (1990). Nuclear Fusion 30, 2545.

Wesson, J.A., A.W. Edwards and R.S. Granetz (1991). Nuclear Fusion 31, 111.

Zakharov, L. and B. Rogers (1992a). MIT Report 92/4.

Zakharov, L. and B. Rogers (1992b). Phys. Fluids 84, 3285.

Appendix I

THE JET TEAM

JET Joint Undertaking, Abingdon, Oxon, OX14 3EA, U.K.

J.M. Adams[1], B. Alper, H. Altmann, A. Andersen[14], P. Andrew, S.Ali-Arshad, W. Bailey, B. Balet, P. Barabaschi, Y. Baranov, P. Barker, R. Barnsley[2], M. Baronian, D.V. Bartlett, A.C. Bell, G. Benali, P. Bertoldi, E. Bertolini, V. Bhatnagar, A.J. Bickley, D. Bond, T. Bonicelli, S.J. Booth, G. Bosia, M. Botman, D. Boucher, P. Boucquey, M. Brandon, P. Breger, H. Brelen, W.J. Brewerton, H. Brinkschulte, T. Brown, M. Brusati, T. Budd, M. Bures, P. Burton, T. Businaro, P. Butcher, H. Buttgereit, C. Caldwell-Nichols, D.J. Campbell, D. Campling, P. Card, G. Celentano, C.D. Challis, A.V.Chankin[23], A. Cherubini, D. Chiron, J. Christiansen, P. Chuilon, R. Claesen, S. Clement, E. Clipsham, J.P. Coad, I.H. Coffey[24], A. Colton, M. Comiskey[4], S. Conroy, M. Cooke, S. Cooper, J.G. Cordey, W. Core, G. Corrigan, S. Corti, A.E. Costley, G. Cottrell, M. Cox[7], P. Crawley, O. Da Costa, N. Davies, S.J. Davies[7], H. de Blank, H. de Esch, L. de Kock, E. Deksnis, N. Deliyanakus, G.B. Denne-Hinnov, G. Deschamps, W.J. Dickson[19], K.J. Dietz, A. Dines, S.L. Dmitrenko, M. Dmitrieva[25], J. Dobbing, N. Dolgetta, S.E. Dorling, P.G. Doyle, D.F. Düchs, H. Duquenoy, A. Edwards, J. Ehrenberg, A. Ekedahl, T. Elevant[11], S.K. Erents[7], L.G. Eriksson, H. Fajemirokun[12], H. Falter, J. Freiling[15], C. Froger, P. Froissard, K. Fullard, M. Gadeberg, A. Galetsas, L. Galbiati, D. Gambier, M. Garribba, P. Gaze, R. Giannella, A. Gibson, R.D. Gill, A. Girard, A. Gondhalekar, D. Goodall[7], C. Gormezano, N.A. Gottardi, C. Gowers, B.J. Green, R. Haange, A. Haigh, C.J. Hancock, P.J. Harbour, N.C. Hawkes[7], N.P. Hawkes[1], P. Haynes[7], J.L. Hemmerich, T. Hender[7], J. Hoekzema, L. Horton, J. How, P.J. Howarth[5], M. Huart, T.P. Hughes[4], M. Huguet, F. Hurd, K. Ida[18], B. Ingram, M. Irving, J. Jacquinot, H. Jaeckel, J.F. Jaeger, G. Janeschitz, Z. Jankowicz[22], O.N. Jarvis, F. Jensen, E.M. Jones, L.P.D.F. Jones, T.T.C. Jones, J-F. Junger, F. Junique, A. Kaye, B.E. Keen, M. Keilhacker, W. Kerner, N.J. Kidd, R. Konig, A. Konstantellos, P. Kupschus, R. Lässer, J.R. Last, B. Laundy, L. Lauro-Taroni, K. Lawson[7], M. Lennholm, J.Lingertat[13], R.N. Litunovski, A. Loarte, R. Lobel, P. Lomas, M. Loughlin, C. Lowry, A.C. Maas[15], B. Macklin, C.F. Maggi[16], G. Magyar, V. Marchese, F. Marcus, J. Mart, D. Martin, E. Martin, R. Martin-Solis[8], P. Massmann, G. Matthews, H. McBryan, G. McCracken[7], P. Meriguet, P. Miele, S.F. Mills, P. Millward, E. Minardi[16], R. Mohanti[17], P.L. Mondino, A. Montvai[3], P. Morgan, H. Morsi, G. Murphy, F. Nave[27], S. Neudatchin[23], G. Newbert, M. Newman, P. Nielsen, P. Noll, W. Obert, D. O'Brien, J. O'Rourke, R. Ostrom, M. Ottaviani, S. Papastergiou, D. Pasini, B. Patel, A. Peacock, N. Peacock[7], R.J.M. Pearce, D. Pearson[12], J.F. Peng[26], R. Pepe de Silva, G. Perinic, C. Perry, M.A. Pick, J. Plancoulaine, J-P. Poffé, R. Pohlchen, F. Porcelli, L. Porte[19], R. Prentice, S. Puppin, S. Putvinskii[23], G. Radford[9], T. Raimondi, M.C. Ramos de Andrade, M. Rapisarda[29], P-H. Rebut, R. Reichle, S. Richards, E. Righi, F. Rimini, A. Rolfe, R.T. Ross, L. Rossi, R. Russ, H.C. Sack, G. Sadler, G. Saibene, J.L. Salanave, G. Sanazzaro, A. Santagiustina, R. Sartori, C. Sborchia, P. Schild, M. Schmid, G. Schmidt[6], H. Schroepf, B. Schunke, S.M. Scott, A. Sibley, R. Simonini, A.C.C. Sips, P. Smeulders, R. Smith, M. Stamp, P. Stangeby[20], D.F. Start, C.A. Steed, D. Stork, P.E. Stott, P. Stubberfield, D. Summers, H. Summers[19], L. Svensson, J.A. Tagle[21], A. Tanga, A. Taroni, C. Terella, A. Tesini, P.R. Thomas, E. Thompson, K. Thomsen, P. Trevalion, B. Tubbing, F. Tibone, H. van der Beken, G. Vlases, M. von Hellermann, T. Wade, C. Walker, D. Ward, M.L. Watkins, M.J. Watson, S. Weber[10], J. Wesson, T.J. Wijnands, J. Wilks, D. Wilson, T. Winkel, R. Wolf, D. Wong, C. Woodward, M. Wykes, I.D. Young, L. Zannelli, A. Zolfaghari[28], G. Zullo, W. Zwingmann.

PERMANENT ADDRESSES

1. UKAEA, Harwell, Didcot, Oxon, UK.
2. University of Leicester, Leicester, UK.
3. Central Research Institute for Physics, Budapest, Hungary.
4. University of Essex, Colchester, UK.
5. University of Birmingham, Birmingham, UK.
6. Princeton Plasma Physics Laboratory, New Jersey, USA.
7. UKAEA Culham Laboratory, Abingdon, Oxon, UK.
8. Universidad Complutense de Madrid, Spain.
9. Institute of Mathematics, University of Oxford, UK.
10. Freien Universität, Berlin, F.R.G.
11. Royal Institute of Technology, Stockholm, Sweden.
12. Imperial College, University of London, UK.
13. Max Planck Institut für Plasmaphysik, Garching, FRG.
14. Risø National Laboratory, Denmark.
15. FOM Instituut voor Plasmafysica, Nieuwegein, The Netherlands.
16. Dipartimento di Fisica, University of Milan, Milano, Italy.
17. North Carolina State University, Raleigh, NC, USA
18. National Institute for Fusion Science, Nagoya, Japan.
19. University of Strathclyde, 107 Rottenrow, Glasgow, UK.
20. Institute for Aerospace Studies, University of Toronto, Ontario, Canada.
21. CIEMAT, Madrid, Spain.
22. Institute for Nuclear Studies, Otwock-Swierk, Poland.
23. Kurchatov Institute of Atomic Energy, Moscow, USSR
24. Queens University, Belfast, UK.
25. Keldysh Institute of Applied Mathematics, Moscow, USSR.
26. Institute of Plasma Physics, Academica Sinica, Hefei, P. R. China.
27. LNETI, Savacem, Portugal.
28. Plasma Fusion Center, M.I.T., Boston, USA.
29. ENEA, Frascati, Italy.

At 1st July, 1992